Physiochemical properties of rat liver mitochondrial ribosomes.

Vinood Patel*
School of Biosciences, University of Westminster

Carol Cunningham
Roy Hantgen
Department of Biochemistry, Wake Forest University School of Medicine

*Vinood Patel was also working for Wake Forest University School of Medicine when this paper was published.

This is an electronic version of an article published in Journal of Biological Chemistry, 276(9), pp. 6739-6746, March 2001. Journal of Biological Chemistry is available online at:

http://www.jbc.org/cgi/content/full/276/9/6739

THE JOURNAL OF BIOLOGICAL CHEMISTRY
Vol. 276, No. 9, Issue of March 2, pp. 6739–6746, 2001

Printed in U.S.A.

Physiochemical Properties of Rat Liver Mitochondrial Ribosomes*

Received for publication, June 30, 2000, and in revised form, December 1, 2000
Published, JBC Papers in Press, December 5, 2000, DOI 10.1074/jbc.M005781200

Vinood B. Patel, Carol C. Cunningham‡, and Roy R. Hantgan

From the Department of Biochemistry, Wake Forest University School of Medicine, Winston-Salem, North Carolina 27157-1016

In the present study, the physiochemical properties of rat liver mitochondrial ribosomes were examined and compared with *Escherichia coli* ribosomes. The sedimentation and translational diffusion coefficients as well as the molecular weight and buoyant density of rat mitochondrial ribosomes were determined. Sedimentation coefficients were established using the time-derivative algorithm (Philo, J. S. (2000) *Anal. Biochem.* 279, 151–163). The sedimentation coefficients of the intact monosome, large subunit, and small subunit were 55, 39, and 28 S, respectively. Mitochondrial ribosomes had a particle composition of 75% protein and 25% RNA. The partial specific volume was 0.688 ml/g, as determined from the protein and RNA composition. The buoyant density of formaldehyde-fixed ribosomes in cesium chloride was 1.41 g/cm^3. The molecular masses of mitochondrial and *E. coli* ribosomes determined by static light-scattering experiments were 3.57 ± 0.14 MDa and 2.49 ± 0.06 MDa, respectively. The diffusion coefficient obtained from dynamic light-scattering measurements was 1.10 ± 0.01 × 10^{-7} cm^2 s^{-1} for mitochondrial ribosomes and 1.72 ± 0.03 × 10^{-7} cm^2 s^{-1} for the 70 S *E. coli* monosome. The hydration factor determined from these hydrodynamic parameters were 4.6 g of water/g of ribosome and 1.3 g/g for mitochondrial and *E. coli* ribosomes, respectively. A calculated hydration factor of 3.3 g/g for mitochondrial ribosomes was also obtained utilizing a calculated molecular mass and the Svedberg equation. These measurements of solvation suggest that ribosomes are highly hydrated structures. They are also in agreement with current models depicting ribosomes as porous structures containing numerous gaps and tunnels.

The mitochondrial genome encodes 13 polypeptides of the oxidative phosphorylation system, 22 tRNAs, and the 12 and 16 S rRNAs (1). Mitochondria DNA deletions or mutations of mitochondrial tRNAs can lead to impairment of polypeptide synthesis and defects in energy production (2, 3). Likewise, in animal models of alcoholic liver disease, chronic ethanol consumption decreases the mitochondrial synthesis of ATP due to lowered concentrations of all 13 polypeptides encoded by the mitochondrial genome (4). However, in this latter case, the depressed functioning of the oxidative phosphorylation system is due to alterations in mitochondrial ribosome function and structure (5, 6). These observations provide another type of mitochondrial disorder that may play a role in pathologies associated with alterations in the mitochondrial protein synthesizing mechanism. Our previous studies demonstrated the need to characterize rat liver mitochondrial ribosomes (mitoribosomes)[1] more rigorously to determine whether alterations in function are accompanied by changes in the physical properties, *i.e.* molecular weight and overall shape. In the present study, a combination of approaches have been employed to determine the physiochemical properties of rat liver mitoribosomes. These included sedimentation velocity measurements with an analytical ultracentrifuge, light-scattering analyses, and electron microscopy.

In previous studies of rat liver mitoribosomes (7–9), the sedimentation coefficient was determined on a sucrose density gradient utilizing *Escherichia coli* ribosomes as a standard. In the present investigation, we have applied a rigorous approach in determining the sedimentation coefficient, namely the time-derivative algorithm as described by Stafford (10) and Philo (11). This procedure has been used to determine the distribution of sedimenting species from sedimentation velocity data obtained in an analytical ultracentrifuge. The time derivative has several advantages when compared with conventional analyses, including a higher signal-to-noise ratio, and the ability to resolve the components of a mixture (10). This latter characteristic was useful in the present study in evaluating whether the intact ribosome dissociated during sedimentation velocity measurements.

Static and dynamic light scattering were employed to measure the molecular weight and translational diffusion coefficient for the rat liver mitoribosomes. The latter parameter can be utilized to determine the Stokes radius of a particle and was employed with electron microscopic analyses to estimate the shape and water content of rat liver mitoribosomes. The light-scattering analyses were particularly useful in this study because measurements can be carried out quickly under conditions that precluded ribosome dissociation. To validate the techniques employed to characterize the rat liver mitoribosomes, we applied the same procedures to characterize the physiochemical properties of the well described *E. coli* ribosome (12, 13).

The sedimentation velocity analyses and the light-scattering measurements revealed a molecular weight for rat liver mitoribosomes that is higher than that reported previously for either rat liver (8) or beef liver (14). This difference in mass between rat and beef liver mitoribosomes is consistent with the

* This work was supported by National Institute on Alcohol Abuse and Alcoholism Grants 02887, 11272, and 00279; by National Science Foundation Grant MCB-9728122; and by the North Carolina Biotechnology Center. The costs of publication of this article were defrayed in part by the payment of page charges. This article must therefore be hereby marked "*advertisement*" in accordance with 18 U.S.C. Section 1734 solely to indicate this fact.

‡ To whom correspondence should be addressed: Dept. of Biochemistry, Wake Forest University School of Medicine, Medical Center Blvd., Winston-Salem, NC 27157-1016. Tel.: 336-716-4254; Fax: 336-716-7671; E-mail: cunn@wfubmc.edu.

[1] The abbreviations used are: mitoribosome, mitochondrial ribosome; $s_{20,w}$, sedimentation coefficient in water at 20 °C; D_t, translational diffusion coefficient; f/f_{min}, frictional ratio; δ_1^{max}, hydration factor; $\bar{\nu}$, partial specific volume; OGDC, α-ketoglutarate dehydrogenase complex; PDC, pyruvate dehydrogenase complex.

earlier finding that only 15% of mitoribosomal proteins had conserved electrophoretic properties (15) and also with the suggestion that mitoribosomal proteins have a high evolutionary rate (15). Furthermore, the present investigation yielded a diffusion coefficient for mitoribosomes, which had not been reported previously. From this parameter an estimation of the solvation was determined, which indicated that these ribosomes are highly hydrated particles.

EXPERIMENTAL PROCEDURES

Materials

Male Sprague-Dawley rats were obtained from Zivic Miller Laboratories, Inc. (Zelienople, PA). Rats were allowed 1 week to acclimatize prior to experimental studies. Ultrapure sucrose was obtained from ICN Pharmaceuticals (Aurora, OH). All other chemicals were of analytical grade.

Methods

Preparation of Mitochondrial Ribosomes—The isolation of ribosomes was as described by Cahill *et al.* (9), except that a mixture of protease inhibitors (phenylmethylsulfonyl fluoride (40 μg/ml), leupeptin (5 μg/ml), pepstatin A (7 μg/ml), and aprotonin (5 μg/ml)) was added to the buffers used in the isolation. After fractionation by sucrose density gradient centrifugation (9), the fraction exhibiting the highest absorbance at 260 nm was collected for subsequent analyses by analytical ultracentrifugation and light-scattering measurements. This fraction typically exhibited a 260 nm/280 nm absorbance ratio of 1.4–1.5. The concentration of ribosomes was determined utilizing an $E^{260}_{0.1\%,\,1\,cm} = 7.5$ (see "Results" for extinction coefficient determination). The activity of purified mitochondrial 55 S ribosomes was measured using a poly(U) directed [^{3}H]phenylalanine polymerization assay as described previously (9), with the exception that activity was measured using ribosomes obtained from the peak maxima of sucrose density gradients.

The purified ribosomes were analyzed for possible contamination with the α-ketoglutarate (OGDC) and pyruvate dehydrogenase complexes (PDC) by monitoring for dehydrogenase activities (16) and dehydrogenase complex subunits by immunoblotting technology (17) employing the Pierce SuperSignal West Pico chemiluminescence kit. Antibody against the E1 subunit of PDC and purified PDC E1 subunit were kindly provided by Dr. M. S. Patel (State University of New York, Buffalo, NY). Dr. G. Lindsay (University of Glasgow, Glasgow, Scotland) generously provided purified OGDC and the antiserum against OGDC.

Preparation of E. coli Ribosomes—*E. coli* ribosomes were prepared according to Rheinberger *et al.* (18) utilizing *E. coli* strain MRE600 (an RNase I$^-$ strain) to minimize ribonuclease levels. Ribosomes were shock-frozen and stored at −80 °C until utilized. For sedimentation velocity analysis in buffer A (30 mM NH_4Cl, 10 mM $MgCl_2$, 10 mM Tris-HCl, pH 7.5, 6 mM β-mercaptoethanol), ribosomes were thawed on ice, diluted with buffer A to give absorbances of 0.7–1.2 units/ml, and subsequently used for analytical ultracentrifugation. For sedimentation velocity analysis in sucrose, ribosomes were immediately loaded onto a 10–30% sucrose gradient prepared in buffer A and centrifuged at 45,000 × g for 14 h in a Beckman SW27 rotor. The gradients were fractionated and absorbances monitored at 260 and 280 nm. Peaks corresponding to purified *E. coli* ribosomes were subsequently used for analytical ultracentrifugation and light-scattering analyses. The concentration of ribosomes was determined utilizing an $E^{260}_{0.1\%,\,1\,cm} = 14.5$ (19, 20). The published value of 0.639 ml/g was used for the partial specific volume ($\bar{\nu}$) (19, 21).

Buoyant Density Analysis in Cesium Chloride—The purified 55 S peak fraction from the sucrose density gradient was dialyzed overnight in buffer B (100 mM KCl, 20 mM $MgCl_2$, 20 mM triethanolamine, pH 7.5, 5 mM β-mercaptoethanol), containing 1% formaldehyde. The refractive index of the sample was measured to ensure no sucrose was present. Buoyant density measurements of formaldehyde-fixed ribosomes in cesium chloride were carried out in buffer B according to Spirin *et al.* (22). This procedure reliably stabilizes ribosomes by fixing the particles with formaldehyde. Inadequate fixation results in loss of ribosomal proteins and artificially high buoyant density values (22). Centrifugation at 187,000 × *g* in a Beckman SW41 Ti rotor was carried out at 4 °C for 48 h. Fractions were collected, and the density was determined according to Ifft *et al.* (23). Absorbance readings of the fractions were measured at 260 nm.

Sedimentation Velocity—Sedimentation velocity experiments were carried out at 4 °C using a Beckman Optima XL-A analytical ultracentrifuge. Bovine serum albumin samples with an absorbance at 280 nm of 0.5, 1.0, and 1.5 were utilized to determine the linearity of the XL-A's optical system. Ribosome boundary movements at a rotor speed of 21,000 rpm, and at fixed time intervals (3 min) as a function of the radius (0.003 radial step size), were obtained over a period of 5 h. Ribosome sample concentrations between 0.05 and 0.16 mg/ml were sufficiently dilute such that they behaved as ideal, noninteracting species.

Data were analyzed by several software applications. First, DCDT+ version 1.02 (Dr. John S. Philo, Thousand Oaks, CA) was applied using the time-derivative algorithm (11). This software was used to analyze sequential files selected to conform to the criteria defined by Stafford (10) to obtain apparent $g(s^*)$ distribution plots of sedimenting species (*i.e.* uncorrected for diffusion). This analysis can also resolve more than one species by fitting the data to a Gaussian function. Second, the Fujita-MacCosham function based on the Lamm equation (24) using the software SVEDBERG, version 6.23 (Dr. John S. Philo, Thousand Oaks, CA) was also employed. This analysis can resolve sedimentation coefficients of more than one species and can fit data obtained over a long time range. Third, the van Holde-Weischet procedure (25) using the software UltraScan 4.1 (Dr. Borries Demeler, University of Texas Health Science Center, Houston, TX) was used to determine the sedimentation coefficient distribution of the sample corrected for diffusion and to provide information on the homogeneity of the sample.

Experimentally determined sedimentation coefficients were corrected for the effects of temperature, solvent density (buffer A, 0.9997 g/cm^3; buffer B, 1.008 g/cm^3) and viscosity (buffer A, 1.57 centipoise; buffer B, 1.57 centipoise). Sedimentation coefficients of samples in sucrose were corrected for solvent density and viscosity as a function of concentration and temperature using standard tables (26). Sedimentation coefficients obtained with the software described above were converted from 4 °C to water at 20 °C to obtain $s_{20,w}$ values (27). The molecular weight of the intact ribosome was calculated from the Svedberg equation (28) utilizing the $s_{20,w}$ and the translational diffusion coefficient (D_t) corrected to water at 20 °C (*i.e.* $D_{20,w}$). The $D_{20,w}$ was obtained from dynamic light-scattering analysis (see below).

Static Light-scattering Analysis—The molecular weight of purified 55 S ribosomes was determined by static light scattering, using a Brookhaven Instrument BI-2030AT correlator, operated together with a BI-200SM light-scattering goniometer/photon counting detector (Brookhaven Instruments, Holtsville, NY) and a Spectra Physics 127 helium-neon laser (35 milliwatts, equipped with a vertical polarization rotator; Spectra Physics, Mountain View, CT) (29, 30). The fraction with maximal absorbance at 260 nm obtained from the sucrose density gradient was used for molecular weight determinations. Light-scattering measurements were made at an angle of 90° in specially formulated microcuvettes (Hellma Cells, Inc., White Plains, NY) maintained at 15 °C in a refractive index matching bath (containing 50% glycerol). Samples were passed through a 0.2-μm filter, with the filtrate collected into acid-washed, dust-free microcuvettes. Intensity measurements from duplicate or triplicate runs were averaged and used for molecular weight calculations. An aliquot of the sample was also utilized for sedimentation velocity studies to provide information on the intactness of the particle. As a consequence, only preparations showing no dissociation were utilized in all analyses. The viscosity and concentration of sucrose in the ribosome sample was determined from the refractive index of sucrose using an Abbe refractometer. Corrections for solvent (*i.e.* sucrose) scattering were obtained by subtracting the intensity measurement determined of blank samples (which had the same sucrose concentration as the ribosome sample) obtained from a control 10–30% sucrose gradient. Sample scattering intensities were expressed relative to a benzene standard (29, 30).

Ribosome concentrations were determined from 260 nm absorbance measurements using an extinction coefficient of mitoribosomes determined from the protein and RNA composition (Ref. 31; see "Results"). The published refractive index increment (dn/dc) for *E. coli* ribosome particles (30, 50, and 70 S) of 0.20 cm^3/g (32) was used in molecular weight calculations. Weight-average molecular weights were determined from the solvent corrected relative scattering intensity (at 90°) using Rayleigh-Gans-Debye theory (33).

Dynamic Light-scattering Analysis—Dynamic light scattering was carried out simultaneously with the same sample used for static light scattering. Measurements were carried out with the detector aperture set at 0.4 or 0.8 mm to optimize the signal to noise ratio (which ranged from 0.13 to 0.25). The intensity-normalized photocount autocorrelation function was used to determine the translational diffusion coefficient D_t by cumulants analysis (33–35). The D_t was corrected for temperature and solvent viscosity to water at 20 °C (*i.e.* $D_{20,w}$) (36). The $D_{20,w}$ was

subsequently employed to determine the particle size (Stokes radius) utilizing the Einstein-Sutherland equation (37). Data analysis of the autocorrelation function also provided an index of the homogeneity of each sample (see "Results"). Additional information about sample heterogeneity was obtained by CONTIN analysis (38) to obtain plots of the distribution of scattering components.

Electron Microscopy—Ribosomes obtained from the peak maxima of sucrose gradients were utilized for electron microscopy. Aliquots of particles were placed on carbon-coated grids and negatively stained with uranyl acetate (39). Micrographs were taken at a magnification of 70,800 with a Phillips 400 transmission electron microscope operated at 80 kev. Particle diameter measurements were randomly recorded from digitized images of 70–100 ribosomes. The length and width of particles were also assessed when ribosomes were orientated in the frontal view.

Unless otherwise stated, results from all experiments are expressed as the mean ± S.E. of six observations.

RESULTS

Sedimentation Velocity: Mitochondrial Ribosomes—The rat liver mitochondrial ribosomes utilized in this study displayed a sucrose density gradient sedimentation profile identical to that reported by Cahill *et al.* (9). The peak absorbance fraction gave a 260:280 ratio of between 1.4–1.5, which is in good agreement with previous observations (9). Since OGDC and PDC complexes have sedimentation coefficients of 36 and 70 S, respectively, the preparation was checked for possible contamination. No pyruvate dehydrogenase activity was detected. Measurement of OGDC activity indicated that 1.4% of the protein in the ribosomal preparation could be this enzyme complex. Analyses of immunoblots were also carried out using purified OGDC and purified E1 subunits of PDC as standards. These analyses suggested that no more than 0.05% and 1.2% of the total protein in the ribosome preparation could be PDC and OGDC, respectively. This indicates that the ribosome preparation is not significantly contaminated with these enzyme complexes, an observation also substantiated by the residual analyses of sedimentation velocity and light-scattering measurements (see below). The translation activity of the purified ribosome, measured by polymerization of phenylalanine, was 0.02 pmol of phenylalanine polymerized/min/pmol of ribosomes. These preparations demonstrated no activity in the absence of soluble translation factors.

The sedimentation properties of ribosome samples taken from the peak maxima at 260 nm of the sucrose gradient were analyzed by various algorithms. Using the time-derivative method, sedimentation data were transformed into an overall distribution of sedimenting species to obtain the $g(s^*)$ plot shown in Fig. 1*A*. Fig. 1*B* shows data from *E. coli* ribosomes that will be discussed in a subsequent section. Fig. 1 *A* demonstrates the application of the DCDT+ analysis, which shows the monosome fitted to a one-species Gaussian distribution centered at 54.0 S with no detectable amounts of its 39 and 28 S subunits. The peak sedimentation coefficient determined by this procedure was 55.1 S (Table I). The ribosome sample in sucrose showed very little dissociation, which was verified with the SVEDBERG analysis that resulted in a single species fit (55 S) from six out of eight preparations. In addition, from the SVEDBERG analysis, the residuals of this typical fit resulted in a root-mean-square deviation of 0.02 absorbance units. A summary of the sedimentation coefficients of ribosomes utilizing the DCDT+ and SVEDBERG software procedures is shown in Table I. In all preparations, the sedimentation coefficient was independent of concentration over the range of 0.05–0.16 mg/ml.

To further validate the DCDT+ analysis procedure, sedimentation velocity data were also analyzed using the van Holde-Weischet method. Fig. 2*A* illustrates absorbance scans taken at fixed time intervals to monitor the movement of sample through the cell. From the extrapolation plot observed in Fig. 2*B*, the convergence of apparent sedimentation coefficients on the *y* intercept indicates that the mitoribosome sample is nearly homogeneous. This finding was reflected in the integral distribution of *s*-values plot (Fig. 2*C*), where 94% of the sample sedimented at ~54–55 S. A small amount of sample (6%) corresponded to dissociated ribosome particles, as verified from the SVEDBERG analysis. There was no evidence of any other particle sedimenting higher than the 55 S monosome. This procedure therefore confirms the findings obtained from the DCDT+ and SVEDBERG analyses.

Two of eight preparations showed the presence of a small fraction sedimenting at 39 S. This was attributed to a minor amount of dissociation in these two preparations. The effect of dissociating the mitochondrial monosome by increasing the potassium and decreasing the magnesium concentrations re-

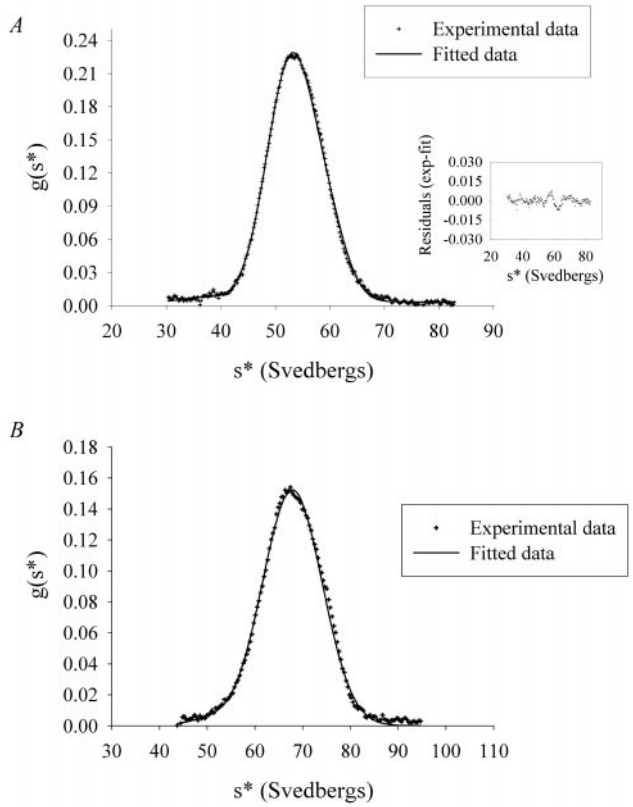

FIG. 1. **A $g(s^*)$ plot of mitochondrial and *E. coli* ribosomes fitted to one-species Gaussian function.** The ribosome sample was taken from the absorbance peak maxima of a 10–30% sucrose density gradient. The sedimentation coefficient distribution (*i.e.* $g(s^*)$) was calculated from the time-derivative algorithm of the concentration profile using the software DCDT+ fitted to a one-species Gaussian function. *A*, mitochondrial ribosomes. The *inset* in *A* pertains to the residuals (difference between the experimental data and the fitted data for each point). The residuals from this typical fit resulted in a root-mean-square deviation of 0.003 absorbance units/Svedberg. *B*, *E. coli* ribosomes.

TABLE I
Summary of sedimentation coefficients of mitochondrial and E. coli ribosomes determined by various software analyses

The numbers in parentheses are the numbers of preparations analyzed.

Analyses	Mitoribosomes	*E. coli*
DCDT+ one-species, peak $s_{20,w}$ value	55.1 ± 0.6 (8)	66.7 ± 0.4 (4)
SVEDBERG one-species, $s_{20,w}$	54.9 ± 0.4 (8)	66.3 ± 0.4 (4)
DCDT+ (dissociated, first species, peak $s_{20,w}$ value)	28.4	
DCDT+ (dissociated, second species, peak $s_{20,w}$ value)	38.9	

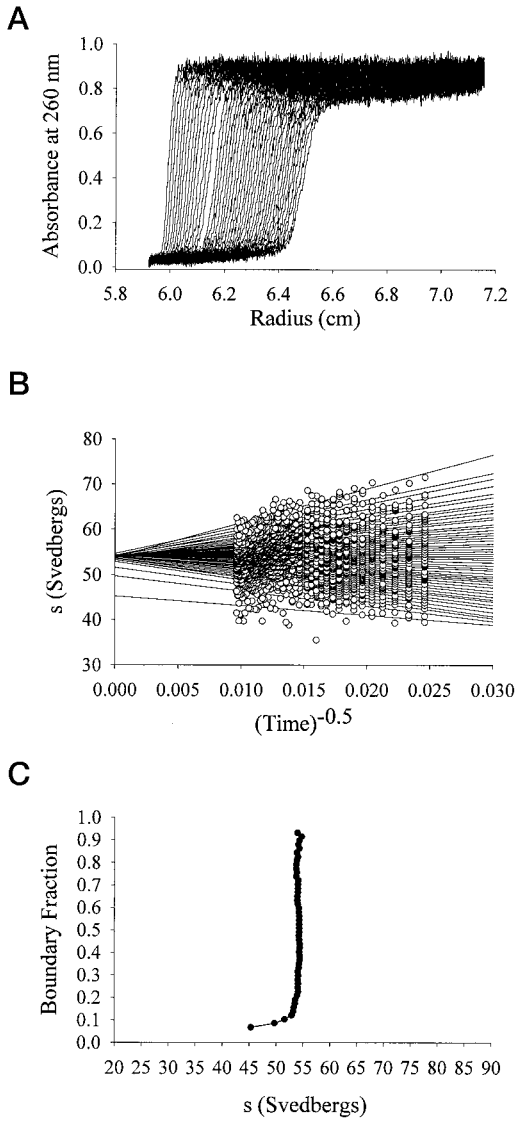

FIG. 2. **van Holde-Weischet analysis of mitoribosomes.** *A*, the particle boundary movement through the cell. The sample was centrifuged in sucrose in an AnTi 60 rotor at 4 °C. Absorbance measurements were taken at fixed time intervals to monitor the sedimentation rate. A period of 5 h at 21,000 rpm was utilized to obtain an adequate number of scans for determination of the sedimentation rate. In this figure representative scans at 3-min intervals are shown. Since a spike was observed in one absorbance scan, this was removed from the analyses. *B*, an extrapolation plot to obtain the diffusion-corrected *S*-values (*y* axis intercept). In this procedure the apparent sedimentation coefficients are extrapolated to infinite time. The 49 absorbance scans shown in Fig. 4*A* were analyzed with 50 equally spaced boundary fractions using the software UltraScan 4.1. *C*, plots of boundary fraction *versus* the corrected *S*-values (from Fig. 4*B*) yielded the integral distribution of sedimentation coefficients.

sulted in two overlapping peaks, with peak sedimentation coefficients of 39 S (large subunit) and 28 S (small subunit) (data not shown). This dissociation pattern is similar to that obtained with bovine liver mitochondrial ribosomes (7).

Sedimentation Velocity: E. coli Ribosomes—The well characterized *E. coli* ribosomes (12, 13, 19, 20) were analyzed in this study to confirm the applicability of the recently developed analyses to mitochondrial ribosomes. *E. coli* ribosomes were applied to sucrose density gradients, and the peak material obtained was subsequently used for sedimentation velocity and light-scattering experiments.

Fig. 1*B* shows a representative $g(s^*)$ plot of *E. coli* ribosomes in sucrose obtained from the peak maxima of density gradients

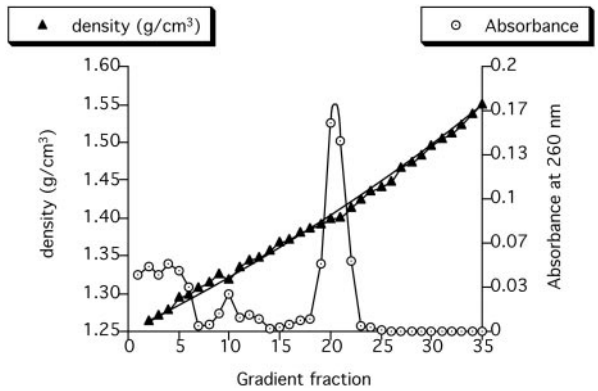

FIG. 3. **Buoyant density measurements of rat mitochondrial ribosomes.** Purified ribosomes were fixed in formaldehyde and centrifuged in a cesium chloride gradient to determine the buoyant density. The gradient formed was from 1.26 to 1.55 g/cm^3. See "Experimental Procedures" for further details.

applying the DCDT+ analysis to a one-species Gaussian fit. In three out of four preparations, a one-species model was obtained from the DCDT+ analysis. The average peak sedimentation coefficient was 67 S, obtained in sucrose (Table I). When analyzed in buffer A, the sedimentation coefficient for *E. coli* ribosomes was 70 S (data not shown). All preparations fitted a single species model in the SVEDBERG analysis. Furthermore, the sedimentation coefficient was independent of concentration over the range utilized (0.05–0.08 mg/ml). A summary of sedimentation coefficients is shown in Table I. Using the van Holde-Weischet procedure, 96% of *E. coli* ribosomes had a sedimentation coefficient of ~67–68 S with a small amount (4%) corresponding to dissociated particles (data not shown).

Mitoribosome Composition, Partial Specific Volume, and Buoyant Density Measurements—The ribosome composition was determined using a mass of rat liver mitochondrial ribosomal proteins of 2.6 MDa (9) and the sum of rat liver mitoribosomal 12 S (0.324 MDa) and 16 S (0.527 MDa) rRNA species (40). Utilizing these values, the protein content was 75% and RNA, 25%. This assumes one molecule of each polypeptide per ribosome and is therefore the minimum amount of protein contained in each ribosome. The low yield of mitoribosomes (1 absorbance unit/ml at 260 nm/25 g of rat liver) precluded direct measurement of $\bar{v}$ and the extinction coefficient. The protein (75%) and RNA (25%) composition was used to determine the ribosome extinction coefficient from the relationship proposed by Hamilton and Ruth (31).

$$E^{260}_{0.1\%,\,1\,cm} = 27 \times (\%\text{RNA}/100) + (\%\text{protein}/100) \qquad \text{(Eq. 1)}$$

An extinction coefficient ($E^{260}_{0.1\%,\,1\,cm}$) of 7.5 was determined from this equation. This value was utilized in calculating ribosome concentrations in the light-scattering measurements. The partial specific volume can be determined from a particle's chemical composition by assuming additivity for the values for RNA (25%) and protein (75%) from the following relationship (31, 41).

$$\bar{v} = (\%\text{RNA})/(100) \times \bar{v}_{\text{RNA}} + (\%\text{protein})/(100) \times \bar{v}_{\text{Protein}} \qquad \text{(Eq. 2)}$$

In Equation 2, $\bar{v}$ = partial specific volume of ribosome, $\bar{v}_{\text{RNA}}$ = 0.53 ml/g (41, 42), and $\bar{v}_{\text{Protein}}$ = 0.74 ml/g (41, 43). A partial specific volume of 0.688 ml/g was calculated from this relationship. This value was compared with the partial specific volume estimated using the reciprocal of the buoyant density determined experimentally for formaldehyde fixed ribosomes. The buoyant density of ribosomes in cesium chloride was 1.41 ± 0.01 g/cm^3 (n = 3) (Fig. 3). In previous studies of ribosomes (41, 43, 44), the inverse of the buoyant density has been utilized to

TABLE II
Summary of physiochemical properties of mitochondrial and E. coli ribosomes

The numbers in parentheses are the numbers of preparations analyzed.

Properties	Mitochondrial	*E. coli*
Molecular mass (MDa)	3.57 ± 0.14 (6)	2.49 ± 0.06 (10)
M_r from Svedberg equation	3.79 ± 0.03 (5)	2.61 ± 0.04 (10)
Diffusion coefficient (10^{-7} cm^2 s^{-1})	1.10 ± 0.01 (6)	1.72 ± 0.03 (10)
Hydrodynamic diameter (nm)	39.1 ± 0.3 (6)	25.1 ± 0.4 (10)
Electron microscopy		
Dimensions (nm)	(26.2 ± 0.4) × (23.6 ± 0.4)	(21.0 ± 0.2) × (19.9 ± 0.2)
Axial ratio	1.11	1.06

estimate the partial specific volume. With the mitoribosomes the reciprocal gave a value of 0.709 ml/g, which is within 3% of the value calculated above. The calculated partial specific volume was utilized in determining $s_{20,w}$ and particle hydration values.

Molecular Weight Determinations for Mitochondrial and E. coli Ribosomes—Molecular weight determinations of mitochondrial and *E. coli* ribosomes obtained from static light-scattering analyses are shown in Table II. The scattering intensity exhibited a linear dependence on concentration over the range utilized (0.03–0.09 mg/ml). Thus, a molecular mass of 3.57 ± 0.14 MDa was obtained for the 55 S mitochondrial monosome. Employing the Svedberg equation and sedimentation coefficients as shown in Fig. 1*A* and diffusion coefficients from the same ribosomal preparation (Fig. 4*B*), the molecular mass was calculated to be 3.79 MDa. Using the calculated weight of ribosomal proteins (9) and the weight of the ribosomal 12 and 16 S RNAs (39), a theoretical mass of 3.45 MDa was determined. This is the minimal value since it assumes one molecule of each of the 86 polypeptides per ribosome (9). The molecular mass of *E. coli* ribosomes determined from light-scattering experiments was 2.49 ± 0.06 MDa (Table II); here also, the scattering intensity was linear with concentration over the range of 0.02–0.26 mg/ml. From the Svedberg equation, a molecular mass of 2.61 MDa was obtained utilizing sedimentation coefficients as shown in Fig. 1*B* and diffusion coefficients from the same ribosome preparation (Fig. 4*B*).

Determination of Diffusion Coefficients by Dynamic Light Scattering—Fig. 4*A* shows the reduced first-order autocorrelation function (29, 33–35), which was used to obtain the translational diffusion coefficient. We routinely analyzed these data with a second order cumulants analysis, as this approach consistently yielded excellent agreement with the experimental data, as shown by the *solid line* in Fig. 4*A*. Size distribution analysis (CONTIN) revealed a narrow distribution of scattering components, as shown by the *inset* in Fig. 4*A*. The translational diffusion coefficients obtained from dynamic light-scattering experiments for mitochondrial and *E. coli* ribosomes were 1.10×10^{-7} cm^2 s^{-1} and 1.72×10^{-7} cm^2 s^{-1}, respectively (Table II). The $D_{20,w}$ was independent of concentration over the range 0.04–0.08 mg/ml for mitochondrial ribosomes (Fig. 4*B*) and 0.02–0.26 mg/ml for *E. coli* ribosomes (Fig. 4*B*) and therefore behaved as an ideal noninteracting system within the above concentration range.

The diameter obtained from calculating the Stokes radius was 39.1 ± 0.3 nm for mitoribosomes and 25.1 ± 0.4 for *E. coli* ribosomes. In both cases the CONTIN analyses indicated that less than 1% of the total sample was present at a diameter greater than 100 nm (see *inset* in Fig. 4*A*). Therefore, it is unlikely that the diameter determined from the $D_{20,w}$ contains a significant contribution from any larger species.

Electron Microscopy of Mitoribosomes and E. coli Ribosomes—Fig. 5*A* shows electron micrographs of negatively stained mitoribosomes. The dimensions were 26.2 nm × 23.6 nm, resulting in an axial ratio of 1.11. For the corresponding *E. coli* ribosomes (Fig. 5*B*), the dimensions were 21.0 nm × 19.9 nm, resulting in an axial ratio of 1.06. In both cases, ribosomes demonstrated a cleft, which delineates the large and small subunits.

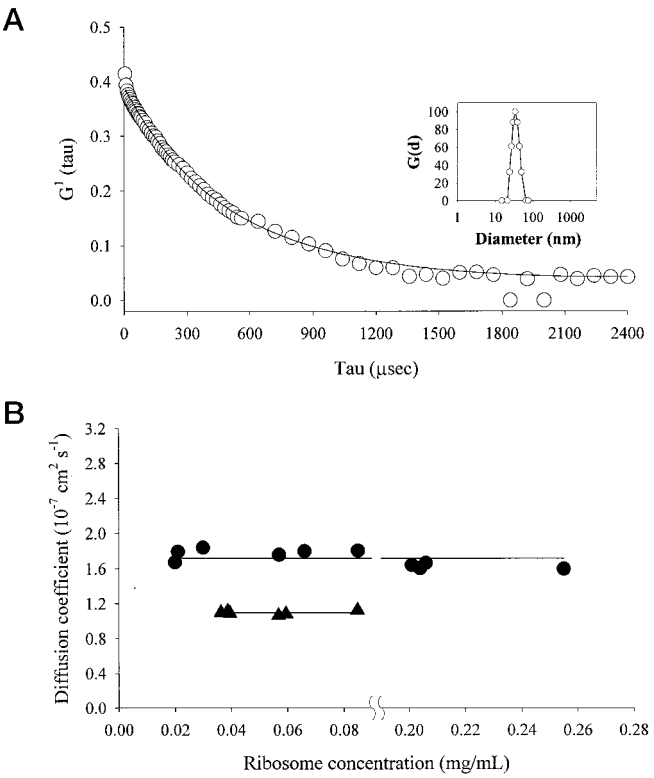

FIG. 4. **Diffusion coefficient measurements of mitochondrial and *E. coli* ribosomes.** Dynamic light-scattering analysis was carried out on ribosomes obtained from the 260-nm absorbance peak of sucrose density gradients. *A*, reduced first-order autocorrelation function for mitoribosomes. The first 64 channels of the BI-2030 correlator were divided into four blocks, each of 16 channels, using sample times of 1, 2, 4, and 8 μs; the last 8 channels were used to define the base line and were extended to 85 ms. Data were collected for 3 min with the detector aperture set at 0.4 or 0.8 mm. Signal/noise ratios of 0.13–0.25 were obtained. The *solid line* corresponds to the autocorrelation function calculated using D_t determined from a second-order cumulant analysis (see "Experimental Procedures"). The *inset* corresponds to intensity distributions of scattering components obtained from CONTIN analysis (38). *B*, translational diffusion coefficients for mitochondrial (*triangles*) and *E. coli* (*circles*) ribosomes. Each point represents the mean of at least two determinations. The *straight line* between each set of data points indicates the mean diffusion coefficient.

DISCUSSION

The aim of the present study was to determine the physiochemical properties of rat liver mitochondrial ribosomes. The molecular weight was measured by light scattering and also by the Svedberg equation with data obtained from sedimentation

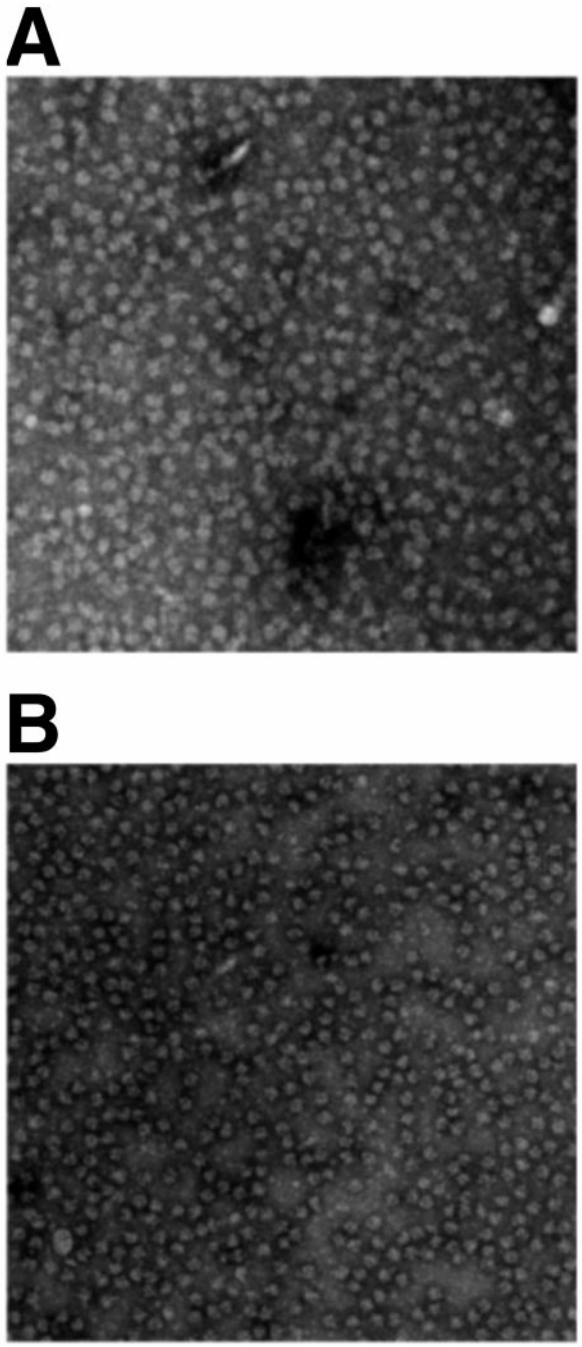

FIG. 5. **Electron micrographs of mitochondrial and *E. coli* ribosomes.** Electron microscopy was carried out on ribosomes obtained directly from the peak maxima of sucrose density gradients. Ribosomes were negatively stained with uranyl acetate and visualized at a magnification of 70,800. *A*, mitochondrial ribosomes. *B*, *E. coli* ribosomes.

velocity and diffusion coefficient measurements. The sedimentation coefficients for the complete monosome, large subunit, and small subunit were 55, 39, and 28 S, respectively, as determined by the time-derivative sedimentation velocity (DCDT+) protocol (11). The other protocols for determining sedimentation coefficients, listed in Table I and Fig. 2, provided $s_{20,w}$ values for the intact monosome very close to that obtained by the DCDT+ analysis. For *E. coli* ribosomes, the sedimentation coefficient of the monosome was ~70 S in buffer and 67 S in sucrose, as indicated by the DCDT+ analyses. These values are the first reports of sedimentation properties of ribosomes using the DCDT+, SVEDBERG, and van Holde-Weischet analyses developed for analytical ultracentrifugation. Additionally, the homogeneity of sample preparations was examined using above mentioned software analyses. In some preparations, a small amount of the 39 S subunit was observed, which never exceeded 6% of the total sample. The van Holde-Weischet analysis also indicated no species larger than the 55 S particle.

The chemical composition of the mitochondrial ribosomes was calculated using the reported mass of rat mitochondrial ribosomal proteins (9) and the particle weights for the rRNA species (40). Based on these data, ribosome particles contained 75% protein and 25% RNA. This is in agreement with the composition determined by chemical analyses of rat liver mitochondrial ribosomes (8, 41). It is also identical to the ratio of rRNA and protein of mitoribosomes from *Xenopus laevis* (45). Because our estimate of the ratio of RNA and protein agreed with the value obtained experimentally (8, 41), we calculated a $\bar{v}$ for rat liver mitoribosomes. This calculated $\bar{v}$ agreed closely with that obtained from buoyant density analysis of mitoribosomes (3% difference), allowing its use in molecular weight determinations.

The calculated molecular mass of the mitochondrial ribosomes from light-scattering experiments was 3.57 MDa, and a similar value of 3.79 MDa was obtained from the sedimentation and diffusion coefficients (Table II). These values are similar to 3.5 MDa obtained for *X. laevis* (45) but are higher than the 3.2 MDa earlier estimated for rat liver (8). In the study by Sacchi *et al.* (8), the molecular weight was estimated from measurements of the RNA content of the ribosome and estimates of the masses of the two rRNAs, which in turn were estimated from molecular weights of cytosolic rRNAs. When the sequences of the rRNAs were established (40), their estimates of the molecular weights of the rRNAs were shown to be too low. This would explain, at least in part, the small difference (<10%) between our measurements of molecular weight and their earlier estimate. The molecular mass determined by sedimentation equilibrium experiments for bovine mitoribosomes has been reported as 2.8 MDa (14), which is significantly lower than the molecular weight obtained in this study for the rat liver mitoribosomes. The difference in molecular weights between bovine and rat liver ribosomes is unlikely to be due to the primary structure of the individual proteins, as analyses to date of mitochondrial ribosomal proteins from different mammalian species indicate significant sequence similarities (46–48).

Since the molecular mass for mitoribosomes obtained in this study by static light scattering was higher than that reported earlier for mitoribosomes from both rat liver (8) and beef liver (14), preparations from *E. coli* were utilized to evaluate the applicability of the light-scattering measurements for analysis of ribosomes. A molecular mass of 2.5 MDa was determined (Table II), which agrees very well with published values of 2.3 MDa (49), 2.5 MDa (50), and 2.6 MDa (19, 20). *E. coli* ribosomes were also analyzed by analytical ultracentrifugation. The molecular mass derived from the Svedberg equation was 2.61 MDa, which is only 4% higher from the value obtained by light scattering. These results suggest that the approaches used provide accurate measures of the molecular mass of rat liver mitoribosomes.

From dynamic light-scattering experiments, we obtained the translational diffusion coefficient. This hydrodynamic parameter, combined with other independently determined physical parameters, was used to determine the frictional ratio using Stokes-Einstein equation. The 55 S ribosome particle has a frictional ratio (f/f_{min}) of 1.97 based on the hydrodynamic diameter (39.1 nm) compared with that of an anhydrous spherical particle diameter (19.8 nm), which indicates either a highly asymmetric and/or highly hydrated structure. If a large particle contaminated the ribosome preparations, then the $D_{20,w}$

would be lower and this would lead to a higher diameter. However, the plots of the distribution of scattering components indicated that less than 1% of the particle was larger than the monosome (see *inset* in Fig. 4*A*). Furthermore, the data from sedimentation velocity experiments suggest that the sample is nearly homogeneous, with only a small amount of dissociation indicated by the presence of the 39 S subunit. Homogeneity was verified by the van Holde-Weischet analysis which gave a precise picture of the *S*-value distribution (25). Aggregation of the ribosome particle could also explain the high frictional ratio. This again appears unlikely, as from our experience rat liver mitoribosomes have a greater tendency to dissociate which would lead to faster moving species and a lower diameter.

In comparison to mitoribosomes, the $D_{20,w}$ for *E. coli* ribosomes was considerably higher (1.72×10^{-7} cm^2 s^{-1}) and agreed closely with published values of 1.71×10^{-7} cm^2 s^{-1} (50, 51), also obtained by dynamic light-scattering measurements. The diameter derived from Stokes-Einstein equation was 25.1 nm, which is also similar to published values for bacterial ribosomes (12, 52). The frictional ratio (f/f_{min}) was 1.46, which corresponded to either an asymmetric structure and/or a hydrated particle. This observed frictional ratio agreed closely with reported (f/f_{min}) values of 1.42 (21), 1.47 (51), and 1.50 (50). Since the observed values for *E. coli* ribosomes corresponded closely with those published previously, this confirms that the dynamic light-scattering measurements used in this study for determining the diameter and frictional ratio for mitoribosomes were reliable.

Electron microscopy images of mitoribosomes revealed a particle with the dimensions of 26.2×23.6 nm, which results in an axial ratio of 1.11. This is similar to the axial ratio (1.06) obtained from analysis of electron microscopy images of *E. coli* ribosomes. The axial ratio obtained for *E. coli* ribosomes by electron microscopy is consistent with the structure established by high resolution cryo-electron microscopy (13, 53), which demonstrates an axial ratio close to unity.

This agreement on overall shape, as demonstrated by electron microscopy of negatively stained particles and cryo-electron microscopy of *E. coli* ribosomes (13, 53), indicates that the images we obtained on negatively stained mitoribosomes reflect their structure in solution. Thus, the electron microscopy indicates that the high frictional ratio obtained by dynamic light scattering cannot be attributed to the overall shape of the particle. The frictional ratio of a particle is also affected by the amount of hydration (δ_1^{max}). If it is assumed that the rat mitoribosome is spherical and that the excess friction can be attributed to hydration, then the δ_1^{max} is 4.5 g of water/g of ribosome, as calculated from the equation $\delta_1^{max} = (\bar{\nu}_2/\bar{\nu}_1[(f/f_{min})^3 - (1.11)]$ (36). Application of the same equation with *E. coli* ribosomes yields a δ_1^{max} of 1.3 g of water/g of ribosome, which agrees with earlier reports of water content determined by independent measurements (19, 54). This agreement validates the approach utilized in this study to estimate hydration of ribosome particles.

Using the measured value for molecular weight determined by static light scattering and the sedimentation coefficient ($s_{20,w}$), a diffusion coefficient was also calculated using the Svedberg equation (28). This calculated $D_{20,w}$ (1.20×10^{-7} cm^2 s^{-1}) is slightly larger (9%) that that obtained from dynamic light scattering (1.10×10^{-7} cm^2 s^{-1}). Utilizing the calculated diffusion coefficient, a value of 3.3 g of water/g of ribosome was estimated. Either of these two estimates of water content for mitoribosomes indicate a highly hydrated particle. It is notable that these estimates of hydration for the mitochondrial ribosome are in the same range as that reported for rat liver cytoplasmic ribosomes (3.7 g/g of ribosome) (55) and its large subunit (3.3 g/g) (56). The degree of hydration of mitoribosomes may explain the finding that, despite possessing a higher molecular weight than *E. coli* ribosomes (Table II), the sedimentation coefficient is much lower (Table I).

In the past decade, there have been major advances in determining the fine structure of the ribosome applying advanced techniques such as electron cryomicroscopy, neutron scattering, small angle x-ray scattering, and x-ray crystallography (12, 13, 52). The structures obtained have provided considerable detail on the relationship between ribosomal structure and the translation mechanism (57, 58). However, there are two diverging views on the compactness of the ribosomal structure. Frank and co-workers propose a rather compact structure (59), whereas van Heel favors a more porous structure, characterized as looking like "a swiss cheese, full of hollows, voids, gaps and tunnels" (58). This porous structure is supported by the recognition that the *E. coli* ribosome has a high water content (18, 54). In this study, we have verified this high level of solvation of *E. coli* ribosomes (1.3 g of water/g of ribosome) using light-scattering techniques. This independent observation of a highly solvated particle provides additional support for the ribosome existing as a porous structure.

Structural analysis of eukaryotic ribosomes suggests the possibility for greater water immobilization than with prokaryotic particles (57, 60), as has been observed in this and earlier studies (55, 56). The outer surface of eukaryotic ribosomes "show more complex extended structures" (57). It is possible that this more complex surface could have the effect of immobilizing water in addition to that which fills a porous structure apparently similar in architecture to that of the prokaryotes (57).

REFERENCES

1. Attardi, G. (1985) *Int. Rev. Cytol.* **93,** 93–143
2. Fromenty, B., Grimbert, S., Mansouri, A., Beaugrand, M., Erlinger, S., Rotig, A., and Pessayre, D. (1995) *Gastroenterology* **108,** 193–200
3. Chinnery, P. F., and Turnbull, D. M. (1999) *Lancet* **354,** S117-S121
4. Coleman, W. B., and Cunningham, C. C. (1990) *Biochim. Biophys. Acta* **1019,** 142–150
5. Coleman, W. B., and Cunningham, C. C. (1991) *Biochim. Biophys. Acta* **1058,** 178–186
6. Cahill, A., Baio, D. L., Ivester, P., and Cunningham, C. C. (1996) *Alcohol Clin. Exp. Res.* **20,** 1362–1367
7. O'Brien, T. W. (1971) *J. Biol. Chem.* **246,** 3409–3417
8. Sacchi, A., Cerbone, F., Cammarano, P., and Ferrini, U. (1973) *Biochim. Biophys. Acta* **308,** 309–403
9. Cahill, A., Baio, D. L., and Cunningham, C. (1995) *Anal. Biochem.* **232,** 47–55
10. Stafford, W. F., III. (1992) *Anal. Biochem.* **203,** 295–301
11. Philo, J. S. (2000) *Anal. Biochem.* **279,** 151–163
12. Svergun, D. I., Burkhardt, N., Pederson-Skov, J., Koch, M. H. J., Volkov, V. V., Kozin, M. B., Merrwink, W., Stuhrmann, H. B., Diedrich, G., and Nierhaus, K. H. (1997) *J. Mol. Biol.* **271,** 588–601
13. Malhotra, A., Penczek, P., Agrawal, R. K., Grassucci, R. A., Junemann, R., Burkhardt, N., Nierhaus, K. H., and Frank, J. (1998) *J. Mol. Biol.* **280,** 103–116
14. Hamilton, M. G., and O'Brien, T. W. (1974) *Biochemistry* **13,** 5400–5403
15. Pietromonaco, S. F., Hessler, R. A., and O'Brien, T. W. (1986) *J. Mol. Evol.* **24,** 110–117
16. Fahien, L. A., and Teller, J. K. (1992) *J. Biol. Chem.* **267,** 10411–10422
17. Towbin, H., Staehelin, T., and Gordon, J. (1979) *Proc. Natl. Acad. Sci. U. S. A.* **76,** 4350–4354
18. Rheinberger, H. J., Geigenmuller, U., Wedde, M., and Nierhaus, K. H. (1988) *Methods Enzymol.* **164,** 658–670
19. Tissieres, A., Watson, J. D., Schlessinger, D., and Hollingworth, B. R. (1959) *J. Mol. Biol.* **1,** 221–233
20. Hill, W. E., Rossetti, G. P., and van Holde, K. E. (1969) *J. Mol. Biol.* **44,** 263–277
21. Allen, S. H., and Wong, K. P. (1979) *Arch. Biochem. Biophys.* **195,** 112–120
22. Spirin, A. S., Belitsina, N. V., and Lerman, M. I. (1965) *J. Mol. Biol.* **14,** 611–615
23. Ifft, J. B., Voet, D. H., and Vinograd, J. (1961) *J. Phys. Chem.* **65,** 1138–1145
24. Philo, J. S. (1996) *Biophys. J.* **72,** 435–444
25. van Holde, K. E., and Weischet, W. O. (1978) *Biopolymers* **17,** 1387–1403
26. Sober, H. A. (1968) *CRC Handbook of Biochemistry,* 1st Ed., Chemical Rubber Co., Cleveland, OH
27. Holladay, L. A., Rivier, J., and Puett, D. (1977) *Biochemistry* **16,** 4895–4900
28. Svedberg, T., and Peterson, K. O. (1940) in *The Ultracentrifuge* (Fowler, R. H., and Kapitza, P., eds) Clarendon Press, Oxford
29. Hantgan, R. R., Braaten, J. V., and Rocco, M. (1993) *Biochemistry* **32,** 3935–3941
30. Hantgan, R. R., Paumi, C., Rocco, M., and Weisel, J. W. (1999) *Biochemistry*

38, 14461–14474
31. Hamilton, M. G., and Ruth, M. E. (1969) *Biochemistry* **8,** 851–856
32. Scafati, A. R., Stornaiuolo, M. R., and Novaro, P. (1971) *Biophys. J.* **11,** 370–384
33. Johnson, C. S., and Gabriel, D. A. (1981) in *Spectroscopy in Biochemistry* (Bell, J. E., ed) Vol. II, pp. 177–272, CRC Press, Boca Raton, FL
34. Koppel, D. E. (1972) *J. Chem. Phys.* **57,** 4814–4820
35. Berne, B. J., and Pecora, R. (1990) *Dynamic Light Scattering with Applications to Chemistry, Biology and Physics*, 4th Ed., R. E. Krieger Publishing Co., Malabar, FL
36. Cantor, C. R., and Schimmel, P. R. (1980) in *Biophysical Chemistry; Part II: Techniques for the Study of Biological Structure and Function*. W. H. Freeman and Co., San Francisco
37. Tanford, C. (1961) *Physical Chemistry of Macromolecules*, pp. 356–365, John Wiley & Sons, New York
38. Provencher, S. W. (1982) *Comp. Phys. Commun.* **27,** 229–242
39. Haschemeyer, R. H., and Meyers, R. J. (1981) in *Principles and Techniques of Electron Microscopy: Biological Applications* (Hayat, M. A., ed) Vol. II, pp. 110–143, University Park Press, Baltimore, MD
40. Gadaleta, G., Pepe, G., De-Candia, G., Quagliariello, C., Sbisa, E., and Saccone, C. (1989) *J. Mol. Evol.* **28,** 497–516
41. Sacchi, A., Ferrini, U., Londei, P., Cammarano, P., and Maraldi, N. (1977) *Biochem. J.* **168,** 245–259
42. Petermann, M. L., and Pavlovec, A. (1966) *Biochim. Biophys. Acta* **114,** 264–276
43. Hamilton, M. G. (1971) *Methods Enzymol.* **20,** 512–521
44. Nieuwenhuysen, P., and Clauwaert, J. (1981) *J. Biol. Chem.* **256,** 9626–9632
45. Leister, D. E., and Dawid, I. B. (1974) *J. Biol. Chem.* **249,** 5108–5118
46. Goldschmidt-Reisin, S., Katakawa, M., Herfurth, E., Wittmann-Liebold, B., Grohmann, L., and Graack, H.-R. (1998) *J. Biol. Chem.* **273,** 34828–34836
47. O'Brien, T. W., Fiesler, S. E., Denslow, N. D., Thiede, B., Wittmann-Liebold, B., Mougey, E. B., Sylvester, J. E., and Graack, H.-R. (1999) *J. Biol. Chem.* **274,** 36043–36051
48. O'Brien, T. W., Liu, J., Sylvester, J. E., Mougey, E. B., Fischel-Ghodsian, N., Thiede, B., Wittmann-Liebold, B., and Graack, H.-R. (2000) *J. Biol. Chem.* **275,** 18153–18159
49. Igarashi, Y., Imamura, T., Suzuki, M., and Miyazawa, Y. (1973) *J. Biochem.* (*Tokyo*) **73,** 683–693
50. Koppel, D. E. (1974) *Biochemistry* **13,** 2712–2719
51. Gabler, R., Westhead, E. W., and Ford, N. C. (1974) *Biophys. J.* **14,** 528–545
52. Cate, J. H., Yusupov, M. M., Yusupova, G. Z., Earnest, T. N., and Noller, H. F. (1999) *Science* **285,** 2095–2104
53. Agrawal, R. K., Lata, R. K., and Frank, J. (1999) *Int. J. Biochem. Cell Biol.* **31,** 243–254
54. Stark, H., Muller, F., Orlova, E. V., Schatz, M., Dube, P., Erdemir, T., Zemilin, F., Brimacombe, R., and van Heel, M. (1995) *Structure* **3,** 815–821
55. Hamilton, M. G., Cavalieri, L. F., and Petermann, M. L. (1962) *J. Biol. Chem.* **237,** 1155–1159
56. Haga, J. Y., Hamilton, M. G., and Petermann, M. L. (1970) *J. Cell Biol.* **47,** 211–221
57. Agrawal, R. K., and Frank, J. (1999) *Curr. Opin. Struct. Biol.* **9,** 215–221
58. van Heel, M. (2000) *Curr. Opin. Struct. Biol.* **10,** 259–264
59. Frank, J., and Agrawal, R. K. (1998) *Biophys. J.* **74,** 589–594
60. Dube, P., Bacher, G., Stark, H., Mueller, F., Zemlin, F., and van Heel, M. (1998) *J. Mol. Biol.* **279,** 403–421